Journal of Solid State Chemistry **147,** 218–228 (1999)
Article ID jssc.1999.8237, available online at http://www.idealibrary.com on IDEAL®

Preparation, Crystal Structures, and Properties of Rhenates with Multiple Re–Re Bonds: Ln_2ReO_5 (Ln = Sm, Eu, Gd), $Ln_3Re_2O_9$ (Ln = Pr, Nd, Sm), and $Ln_4Re_6O_{19}$ (Ln = La–Nd)

Wolfgang Jeitschko, Dieter H. Heumannskämper, Marietta S. Schriewer-Pöttgen, and Ute Ch. Rodewald

Anorganisch-Chemisches Institut, Universität Münster, Wilhelm-Klemm-Strasse 8, D-48149 Münster, Germany

Received October 13, 1998; in revised form February 14, 1999; accepted February 28, 1999

IN MEMORY OF JEAN ROUXEL

Most of the title compounds were prepared by reaction of the rare-earth metaperrhenates $Ln(ReO_4)_3$ with the rare-earth metals in sealed silica tubes. $Nd_4Re_6O_{19}$ was obtained by reaction of the intermetallic compound $NdRe_2$ with the metaperrhenate $Nd(ReO_4)_3$. The compounds Ln_2ReO_5 crystallize with a tetragonal structure ($P4/n$, $Z = 4$), which was determined from four-circle X-ray diffractometer data of twinned crystals of Eu_2ReO_5 [$a = 861.0(4)$ pm, $c = 574.3(3)$ pm] and refined for Gd_2ReO_5 [$a = 858.8(4)$ pm, $c = 569.6(2)$ pm]. The compounds $Ln_3Re_2O_9$ are isotypic with $La_3Re_2O_9$, however, with somewhat differing oxygen coordination of the rare-earth atoms, as was shown by a structure refinement from single-crystal data of $Sm_3Re_2O_9$ [$P\bar{1}$, $a = 551.8(1)$ pm, $b = 678.8(2)$ pm, $c = 1086.7(3)$ pm, $\alpha = 76.57(1)^\circ$, $\beta = 75.56(2)^\circ$, $\gamma = 68.66(1)^\circ$]. The rhenates $Ln_4Re_6O_{19}$ have a structure first determined for $La_4Re_6O_{19}$. The rhenium atoms in the compounds Ln_2ReO_5, with the oxidation number +4, are paired with a formal Re–Re triple bond (225 pm) in a square-antiprismatic oxygen coordination (Re_2O_8). In $Sm_3Re_2O_9$ two kinds of Re_2 pairs are present. The Re(IV) pairs with a formal triple bond have again a Re–Re distance of 225 pm. They are situated in a tetragonal prism of oxygen atoms. The other rhenium atoms, with oxidation number +5, have octahedral oxygen coordination. They form pairs via a common edge of their oxygen octahedra with a formal double bond of 242 pm. The magnetic properties of these compounds indicate that the rhenium atoms do not carry any substantial magnetic moments. The crystal structures of the reduced oxorhenates of the rare-earth elements are briefly reviewed. The Re–Re bond lengths correlate with the formal bond order deduced from the oxidation states.

INTRODUCTION

Oxorhenates of the rare earth elements have been investigated for many years. A brief survey of the early literature has been given by Muller and Roy (1). In the perrhenates Y_3ReO_8 (2), La_3ReO_8 (3, 4), and Sm_3ReO_8 (5), the Re(VII) atoms are octahedrally coordinated by oxygen atoms, while the high temperature modification of the isotypic rare-earth metaperrhenates $Ln(ReO_4)_3$ (Ln = Y, Eu–Yb) contain tetrahedral ReO_4 groups (6–8). In $La_3Re_2O_{10}$ the rhenium atoms have the oxidation number +5.5. They are situated in edge-sharing oxygen octahedra, thus forming pairs with a Re–Re distance of 248.4 pm (9). This is also the coordination of the Re_2 pairs in $Nd_4Re_2O_{11}$ (10), where the rhenium atoms have the oxidation number +5. Edge-sharing ReO_6 octahedra are also found for the Re_2 pairs in $Dy_5Re_2O_{12}$ (11, 12) and $Ho_5Re_2O_{12}$ (13) with rhenium in the oxidation state +4.5, and also for $La_4Re_6O_{19}$ (14, 15), where the rhenium atoms have the oxidation number +4.33. Here we report about the compounds $Ce_4Re_6O_{19}$, $Pr_4Re_6O_{19}$, and $Nd_4Re_6O_{19}$, which are isotypic with $La_4Re_6O_{19}$ and which we have briefly already introduced at a conference (16).

When the rhenium atoms have still lower oxidation numbers, they also form pairs. However, these Re_2 pairs are situated in tetragonal prisms or antiprisms. A tetragonal prism of oxygen atoms occurs in the structure of La_2ReO_5 (17), where the rhenium atoms are in the oxidation state +4 with a Re–Re distance of 226.2 pm. In $La_3Re_2O_9$ (18) two kinds of Re_2 pairs are found, one within edge-shared oxygen octahedra and the other with tetragonal prismatic oxygen environment. These may be assigned the oxidation states +5 and +4, respectively, with Re–Re distances of 245.6 and 223.5 pm. The compounds $Ln_3Re_2O_9$ (Ln = Pr, Nd, Sm) reported in the present paper may be considered to be isotypic with $La_3Re_2O_9$, although there are differences in the coordination numbers of the rare-earth atoms. Tetragonal antiprismatic coordination is found for the Re_2 pairs in the structures of Eu_2ReO_5 and Gd_2ReO_5, which were presented at a conference (19) and which are fully published

0022-4596/99 $30.00

here. In the meantime the structure of the compound Sm_2ReO_5 has been reported by Wltschek, Paulus, Ehrenberg, and Fuess (20), which is isotypic with that of the europium and gadolinium compounds. We have also investigated the magnetic properties of some of these reduced rhenates.

SAMPLE PREPARATION AND LATTICE CONSTANTS

Most of the samples were prepared by reaction of the rare-earth metals with the corresponding metaperrhenates $Ln(ReO_4)_3$. The light rare-earth elements (nominal purities all $>99.9\%$) were purchased in the form of filings and stored under dry (Na) paraffin oil, which was washed away by dry hexane prior to the reactions. Europium was purchased as an ingot, and filings were prepared under oil and cleaned from adhering iron particles by a magnet.

The metaperrhenates were prepared by reaction of the lanthanoid oxides ($>99.9\%$) and an excess of elemental rhenium in the form of powder (Starck, $>99.9\%$). The mixtures were annealed in one-sided open silica tubes (30 cm) at 450°C for 2 days. The excess rhenium was condensed at the cold parts of the tubes (outside the furnace) in the form of Re_2O_7. The metaperrhenates have a tendency to hydrate on air. They were dried in open silica tubes at 400°C (1 hour) prior to the reactions.

The rare-earth elements were annealed with the metaperrhenates in molar ratios varying between 1 : 1 and 3 : 1 with a total weight of ca. 300 mg in evacuated sealed silica tubes at temperatures of about 1000–1200°C and annealing times of 5–10 days. After quenching in air, the excess metaperrhenate flux was washed away with ethanol and the products were dried at 110°C in air. $Nd_4Re_6O_{19}$ was prepared by reaction of an arc-melted alloy of $NdRe_2$ in powdered form with the powder of the metaperrhenate $Nd(ReO_4)_3$. The powders were sealed in an evacuated silica tube and annealed for 10 days at 1050°C.

The products were generally obtained in well-crystallized form with black color. They are stable in air for long periods of time. Energy dispersive X-ray fluorescence analyses of the samples in a scanning electron microscope did not show any impurity elements heavier than sodium.

TABLE 1
Lattice Constants of Tetragonal Oxides with Eu_2ReO_5 Type Structure[a]

Compound	a (pm)	c (pm)	V (nm^3)	Reference
Sm_2ReO_5	864.6	575.4	0.4301	1
Sm_2ReO_5	864.6(3)	574.7(2)	0.4296	20
Sm_2ReO_5	864.2(1)	575.0(1)	0.4294	This work
Eu_2ReO_5	861.0(4)	574.3(3)	0.4257	This work
Gd_2ReO_5	858.7	570.4	0.4206	1
Gd_2ReO_5	858.8(4)	569.6(2)	0.4201	This work

[a] Standard deviations in the place values of the least significant digits are given in parentheses for all crystallographic data throughout the paper.

All samples were characterized by their Guinier powder patterns with Cu$K\alpha_1$ radiation and α-quartz as an internal standard ($a = 491.30$ pm, $c = 540.46$ pm). To facilitate the proper assignement of indices, the experimental patterns were compared with the ones calculated (21) using the positional parameters obtained from the single-crystal investigations. The lattice constants (Tables 1–3) were obtained by least-squares fits.

MAGNETIC PROPERTIES

The magnetic susceptibilities of Eu_2ReO_5 and Gd_2ReO_5 were determined with a SQUID (superconducting quantum interference device) magnetometer (Quantum Design, Inc.) at a magnetic flux density of 0.5 T between 2 and 300 K. At temperatures above 100 K the $1/\chi$ vs. T plot for Eu_2ReO_5 suggests Curie–Weiss behavior (Fig. 1). However, the strong temperature dependence of the susceptibility at lower temperatures indicates Van Vleck paramagnetism, which is frequently observed for Eu^{3+} compounds. The data were corrected for the core diamagnetism. The magnetic moment calculated according to the equation $\mu_{exp} = 2.83\,[(\chi/2) \times T]^{1/2}\,\mu_B$ amounts to $\mu_{exp} = 3.6(1)\,\mu_B$ for 300 K. This value is in good agreement with the theoretical value of $\mu_{eff} = 3.51\,\mu_B$ calculated for Eu^{3+} with Van Vleck's formula for 293 K with a screening constant of $\sigma = 34$ (22).

TABLE 2
Lattice Constants for the Standardized Setting of $La_3Re_2O_9$ Type Compounds

Compound	a (pm)	b (pm)	c (pm)	α (°)	β (°)	γ (°)	V (nm^3)	Reference
$La_3Re_2O_9$	567.3(4)	685.8(5)	1112.8(7)	76.4(2)	75.9(2)	68.8(2)	0.3863	18
$Pr_3Re_2O_9$	560.4(1)	681.1(1)	1101.6(2)	76.91(1)	75.56(1)	69.02(1)	0.3758	This work
$Nd_3Re_2O_9$	557.2(6)	680.1(6)	1096.8(1)	76.83(1)	75.56(1)	68.89(1)	0.3711	This work
$Sm_3Re_2O_9$	551.8(1)	678.8(2)	1086.7(3)	76.57(1)	75.56(2)	68.66(1)	0.3626	This work
$Sm_3Re_2O_9$[a]	550.7(1)	677.7(1)	1084.8(2)	76.60(1)	75.57(2)	68.64(1)	0.3607	This work

[a] These lattice constants were obtained on the four-circle diffractometer. For the calculation of the interatomic distances, the lattice constants from the powder data were used.

TABLE 3
Lattice Constants of Cubic Oxides with $La_4Re_6O_{19}$ Type Structure

Compound	a (pm)	V (nm^3)	Reference
$La_4Re_6O_{19}$	903.25(14)	0.7369	14
$La_4Re_6O_{19}$	903.08(2)	0.7365	15
$La_4Re_6O_{19}$	903.44(9)	0.7374	This work
$Ce_4Re_6O_{19}$	899.78(7)	0.7285	This work
$Pr_4Re_6O_{19}$	896.59(2)	0.7207	This work
$Nd_4Re_6O_{19}$	894.05(8)	0.7146	This work

Gd_2ReO_5 shows Curie–Weiss behavior down to 10 K. The susceptibility data were fitted to the modified Curie–Weiss law $\chi = \chi_0 + C/(T - \Theta)$. From the expression $\mu_{exp} = (8C)^{1/2}\,\mu_B$ we obtained a magnetic moment of $\mu_{exp} = 7.79\ (\pm 0.05)\ \mu_B$ per gadolinium atom, in good agreement with the theoretical moment of 7.94 μ_B calculated for a free Gd^{3+} ion from the relation $\mu_{eff} = g[J(J+1)]^{1/2}\,\mu_B$. The small difference may be ascribed to crystal field effects.

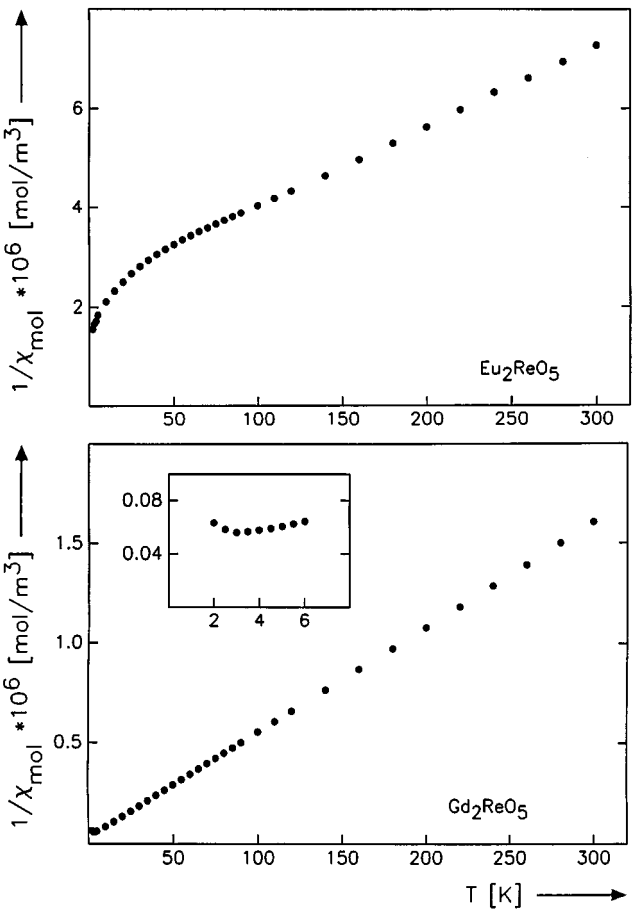

FIG. 1. Temperature dependence of the reciprocal susceptibilities of Eu_2ReO_5 and Gd_2ReO_5.

The negative Weiss constant $\Theta = -5.4\ (\pm 0.3)$ K suggests antiferromagnetic order, and the minimum in the reciprocal susceptibility curve at low temperature suggests a Néel temperature of $T_N = 3.0\ (\pm 0.5)$ K. The temperature independent term of the magnetic susceptibility $\chi_0 = -174\ (\pm 90) \times 10^{-6}$ cm^3 per formula unit (f.u.) is negative, reflecting the core diamagnetism of the compound.

The magnetic properties of the compounds $Ln_4Re_6O_{19}$ (Ln = La, Ce, Pr, Nd) were determined with a Faraday balance as described earlier (23). The magnetic susceptibilities of the compounds $Ce_4Re_6O_{19}$, $Pr_4Re_6O_{19}$, and $Nd_4Re_6O_{19}$ show Curie–Weiss behavior (Fig. 2). The data were evaluated with the modified Curie–Weiss law as described above, resulting in magnetic moments μ_{exp} of 2.38 (± 0.04), 3.33 (± 0.7), and 3.58 (± 0.4) μ_B per lanthanoid atom, in good agreement with the theoretical moments μ_{eff} of 2.54, 3.58, and 3.62 μ_B calculated for the free ions Ce^{3+}, Pr^{3+}, and Nd^{3+}, respectively. The small differences between the experimental and the theoretical moments may again be ascribed to crystal field effects. The negative Weiss constants Θ of $-20\ (\pm 5)$, $-47\ (\pm 8)$, and $-29\ (\pm 4)$ K suggest antiferromagnetic order of the lanthanoid moments at low temperatures. The temperature-independent terms χ_0 of the magnetic susceptibilities obtained by these least-squares fits are very small: $+140\ (\pm 250)$, $-480\ (\pm 500)$, and $+260\ (\pm 350) \times 10^{-6}$ cm^3/f.u. for $Ce_4Re_6O_{19}$,

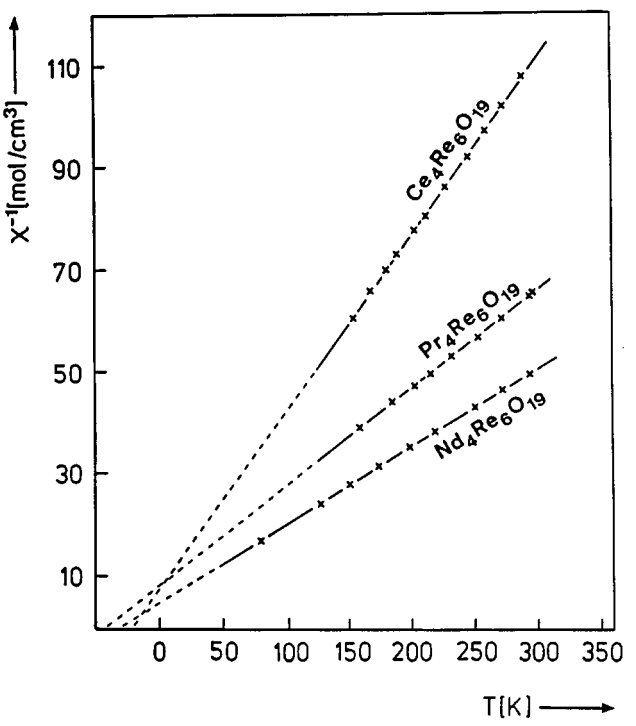

FIG. 2. Reciprocal susceptibilities of the compounds $Ln_4Re_6O_{19}$ (Ln = Ce, Pr, Nd) as a function of temperature. The dashed lines show linear extrapolations to zero reciprocal susceptibility.

$Pr_4Re_6O_{19}$, and $Nd_4Re_6O_{19}$, respectively. The absolute values of these terms are all less than 2% of the total susceptibilities, and therefore these values have large error limits. However, for the isotypic compound $La_4Re_6O_{19}$, where the lanthanum atoms do not carry moments, a much more accurate corresponding value of the susceptibility could be determined. Several measurements at different magnetic flux intensities at room temperature varied between -20×10^{-6} and $+20\times10^{-6}$ cm^3/f.u. This result will discussed below.

CRYSTAL STRUCTURES

Crystals of Eu_2ReO_5, Gd_2ReO_5, and $Sm_3Re_2O_9$ were isolated from the samples in an ultrasonic bath with ethanol. They were investigated in Buerger precession and Weissenberg cameras to establish their symmetry and suitability for the intensity data collections. The intensity data were collected on a four-circle diffractometer using graphite-monochromated Mo$K\alpha$ radiation, a scintillation counter with pulse-height discrimination, $\theta/2\theta$ scans, and background counts at both ends of each scan. Absorption corrections were made from psi scan data. Further details about the data collections are summarized in Table 4. Most of the programs used for solving and refining the structures were taken from the SDP program system (24).

The structure of Eu_2ReO_5 was solved by direct methods, which resulted in the metal atom positions. The oxygen atoms were located by difference Fourier syntheses. The least-squares refinement in the space group $P4/n$ resulted in residual electron density peaks close to the rhenium positions, which eventually could be rationalized by twinning. The reciprocal lattice was clearly of the low Laue symmetry $4/m$; however, the intensity distribution simulated to some extent the higher symmetry $4/mmm$, which could result from a twin with the matrix (010, 100, 00$\bar{1}$). The structure was then refined with a least-squares program, which accounted for this twinning (25). A twin ratio of 0.693(5) : 0.307(5) was obtained. The same difficulty was encountered with the structure refinement of the isotypic compound Gd_2ReO_5. This structure was eventually refined with the program SHELXL-92 (26), again accounting for the twinning, which resulted in a twin ratio of 0.784(5):0.216(5).

One rhenium position of $Sm_3Re_2O_9$ was obtained from a Patterson synthesis. The other metal positions and finally also the oxygen positions were determined by difference Fourier syntheses. All structures were refined with atomic scattering factors, corrected for anomalous dispersion, as provided by the programs. Parameters accounting for isotropic secondary extinction were optimized as least-squares variables. The structures of Eu_2ReO_5 and Gd_2ReO_5 were refined with anisotropic displacement parameters for the metal atoms and isotropic displacement parameters for the oxygen atoms. In the final least-squares cycles for $Sm_3Re_2O_9$, all atoms had anisotropic displacement parameters. The lattice constants of the $La_3Re_2O_9$ type compounds (Table 2) and the positional parameters of all structures were standardized by the program STRUCTURE TIDY (27). Final residuals and atomic parameters are summarized in Tables 4, 5, and 6, and the interatomic

TABLE 4
Crystal Data for Eu_2ReO_5, Gd_2ReO_5, and $Sm_3Re_2O_9$

Compound	Eu_2ReO_5	Gd_2ReO_5	$Sm_3Re_2O_9$
Space group	$P4/n$	$P4/n$	$P\bar{1}$
Formula units/cell (Z)	4	4	2
Formula mass	570.1	580.7	1934.9
Calculated density (g/cm^3)	8.893	9.175	8.861
Crystal dimensions (μm^3)	$40\times40\times78$	$40\times40\times20$	$33\times40\times84$
$\theta/2\theta$ scans up to 2θ	90°	72°	80°
Range in h, k, l	±17, ±17, 0–11	±14, ±14, 0–9	±9, ±12, ±19
Total number of reflections	7498	4729	8914
Unique reflections	1888	1075	4457
Inner residual	0.046	0.038	0.030
Reflections with $I_0 > 3\sigma(I_0)$	1251	743	3426
Number of variables	28	28	128
Conventional residual (R_F)	0.025	0.020	0.026

TABLE 5
Atomic Parameters of Eu_2ReO_5 and Gd_2ReO_5

Atom	$P4/n$	x	y	z	U^a
			Eu_2ReO_5		
Eu	8g	0.09970(4)	0.60832(4)	0.24952(8)	47.6(5)
Re1	2c	1/4	1/4	0.1497(1)	38.9(7)
Re2	2c	1/4	1/4	0.54267(9)	37.5(9)
O1	8g	0.0501(7)	0.1577(7)	0.601(67)	68(9)
O2	8g	0.1579(7)	0.0515(7)	0.102(1)	73(9)
O3	2b	1/4	3/4	1/2	56(12)
O4	2a	1/4	3/4	0	64(13)
			Gd_2ReO_5		
Gd	8g	0.10017(4)	0.60842(4)	0.24962(8)	42.6(5)
Re1	2c	1/4	1/4	0.1497(1)	35(7)
Re2	2c	1/4	1/4	0.5439(1)	31(1)
O1	8g	0.0501(6)	0.1591(6)	0.603(1)	43(10)
O2	8g	0.1573(7)	0.0501(7)	0.099(1)	68(11)
O3	2b	1/4	3/4	1/2	43(17)
O4	2a	1/4	3/4	0	93(20)

[a]The last column contains the isotropic U values of the oxygen and the equivalent isotropic U values (pm^2) of the anisotropic thermal parameters of the metal atoms.

TABLE 6
Atomic Parameters of $Sm_3Re_2O_9$[a]

Atom	*x*	*y*	*z*	*U*
Sm1	0.01037(6)	0.21233(5)	0.26936(3)	59(1)
Sm2	0.22402(6)	0.16144(5)	0.88320(3)	63(1)
Sm3	0.29607(6)	0.60352(5)	0.37151(3)	55(1)
Re1	0.34576(5)	0.12607(3)	0.56895(2)	36(1)
Re2	0.51563(5)	0.38486(3)	0.09296(2)	37(1)
O1	0.0587(9)	0.1144(7)	0.7203(4)	56(7)
O2	0.0759(10)	0.2111(9)	0.4738(5)	111(9)
O3	0.1808(10)	0.4993(8)	0.1973(5)	85(8)
O4	0.2875(10)	0.4212(7)	0.5811(5)	93(8)
O5	0.3886(10)	0.1721(7)	0.0702(5)	78(7)
O6	0.5851(10)	0.0714(7)	0.6894(4)	62(7)
O7	0.5951(10)	0.1904(7)	0.4054(5)	80(8)
O8	0.6523(10)	0.5241(7)	0.1823(5)	62(7)
O9	0.8673(10)	0.1881(7)	0.0608(5)	72(7)

[a] All atoms are situated on the general position (2*i*) of space group $P\bar{1}$. All were refined with anisotropic thermal parameters. The last column contains the equivalent isotropic parameters *U* (pm^2).

distances are given in Tables 7 and 8. The structure factors of Eu_2ReO_5 and $Sm_3Re_2O_9$ are listed in Ref. (28), and those of Gd_2ReO_5 in Ref. (29).

TABLE 7
Interatomic Distances in the Structures of Ln_2ReO_5 (Ln = Eu, Gd)[a]

		Eu_2ReO_5	Gd_2ReO_5
Ln:	O4	228.4	227.1
	O3	228.7	227.3
	O1	242.9	243.2
	O2	244.0	240.5
	O2	247.9	247.6
	O1	248.7	248.2
	O1	254.2	252.1
	O2	264.0	263.2
Re1:	4O2	190.4	191.4
	Re2	225.7	224.5
Re2:	4O1	192.5	191.6
	Re1	225.7	224.5
O1:	Re2	192.5	191.6
	Ln	242.9	243.2
	Ln	248.7	248.2
	Ln	254.1	252.1
O2:	Re1	190.4	191.4
	Ln	244.0	240.5
	Ln	247.9	247.6
	Ln	264.0	263.2
O3:	4*Ln*	228.7	227.3
O4:	4*Ln*	228.4	227.1

[a] All lanthanoid– and rhenium–oxygen distances shorter than 390 and 310 pm, respectively, are listed. The shortest metal–rhenium distances are 339 pm (Eu–Re) and 338 pm (Gd–Re). Standard deviations are all 0.6 pm, or less.

TABLE 8
Interatomic Distances in the Structure of $Sm_3Re_2O_9$[a]

Sm1:	O2	233.6	Re1:	O2	186.7	O4:	Re1	194.1
	O3	235.5		O4	194.1		Sm3	232.4
	O1	235.6		O6	196.8		Sm3	241.7
	O6	242.1		O1	198.8		Sm1	301.7
	O7	243.2		O7	201.4		Sm3	319.2
	O8	249.8		O7	202.5		Sm2	334.6
	O5	259.3		Re1	242.3	O5:	Re2	190.5
	O9	263.5	Re2:	O3	190.3		Sm2	244.8
	O4	301.7		O5	190.5		Sm2	253.7
	O2	359.0		O9	191.4		Sm1	259.3
Sm2:	O1	231.3		O8	192.7	O6:	Re1:	196.8
	O8	237.5		Re2	225.1		Sm1	242.1
	O9	237.5	O1:	Re1	198.8		Sm3	242.8
	O5	244.8		Sm1	231.3		Sm2	253.0
	O9	251.0		Sm2	235.6	O7:	Re1	201.4
	O6	253.0		Sm3	241.9		Re1	202.5
	O5	253.7	O2:	Re1	186.7		Sm1	243.2
	O3	271.2		Sm1	233.6		Sm3	267.9
	O4	334.6		Sm3	245.1		Sm3	333.3
Sm3:	O4	232.4		Sm3	318.0	O8:	Re2	192.7
	O4	241.7		Sm1	359.0		Sm2	237.5
	O1	241.9	O3:	Re2	190.3		Sm3	247.2
	O6	242.8		Sm1	235.5		Sm1	249.8
	O2	245.1		Sm3	245.8	O9:	Re2	191.4
	O3	245.8		Sm2	271.1		Sm2	237.5
	O8	247.2					Sm2	251.0
	O7	267.9					Sm1	263.5
	O2	318.0						
	O4	319.2						
	O7	333.3						

[a] All Sm–O distances shorter than 380 pm and all Re–O distances shorter than 315 pm are listed. Standard deviations are all 0.5 pm or less.

DISCUSSION

In the rare-earth oxorhenates reported here the rhenium atoms all have oxidation states of less than +7. They crystallize with three different structure types. The rhenates Sm_2ReO_5, Eu_2ReO_5, and Gd_2ReO_5 are isotypic. We will refer to them as Eu_2ReO_5 type compounds since the structure of Eu_2ReO_5 was determined first (19), even though a full account of this work is given only here. The structure of the isotypic samarium rhenate Sm_2ReO_5 has been determined independently (20). The other compounds reported here crystallize with structures that have been determined first for $La_3Re_2O_9$ (18) and $La_4Re_6O_{19}$ (11, 12). In the $La_3Re_2O_9$ type compounds, all oxygen atoms are coordinated to at least one rhenium atom. In contrast, the structures of Eu_2ReO_5 and $La_4Re_6O_{19}$ contain some oxygen atoms, which are surrounded solely by rare-earth atoms. In Eu_2ReO_5 these are the O3 and O4 atoms. They are situated in tetrahedra formed by the europium atoms (Fig. 3). These Eu_4O tetrahedra share edges, thus forming chains that extend along the *z* axis (Fig. 4). In the structure

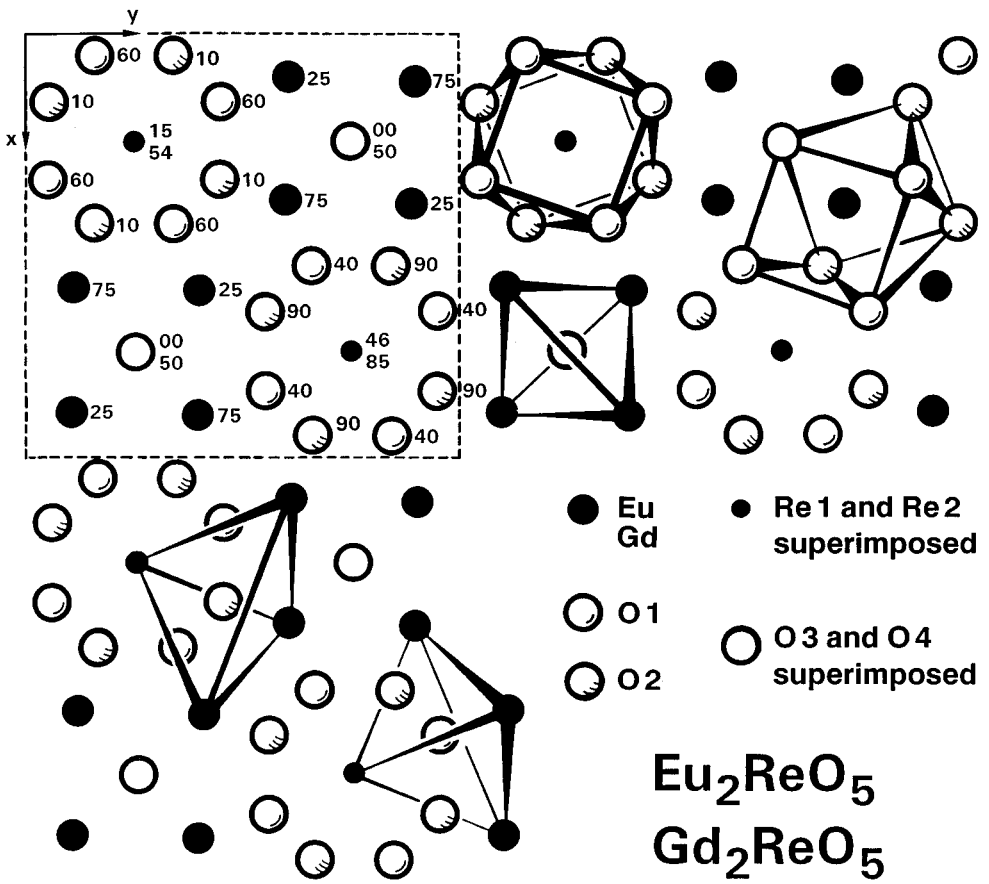

FIG. 3. The isotypic structures of Eu_2ReO_5 and Gd_2ReO_5 projected along the fourfold axis. The coordination polyhedra of all atoms are shown. Note that the Re1 and Re2 atoms of the Re_2O_8 groups are superimposed. Similary, only one of the superimposed O3 and O4 atoms in the coordination polyhedron of the rare-earth atoms (with coordination number 8) is visible. In the upper left-hand corner the heights of the atoms in the projection direction are given in hundredths.

of $La_4Re_6O_{19}$ the O3 atoms (one-nineteenth of all oxygen atoms) are surrounded solely by lanthanum atoms, again forming La_4O tetrahedra. However, these tetrahedra are not connected to each other (Fig. 5).

In looking at the projection of the structure of Eu_2ReO_5 (Fig. 3) one is tempted to believe that the Laue symmetry of this compound is 4/*mmm* and not 4/*m*. Indeed, the europium and oxygen atoms have atomic positions that are almost compatible with the space group *P*4/*ncc* (No. 130). Only the rhenium positions violate this space group and lower the symmetry from *P*4/*ncc* to *P*4/*n*. They would also be compatible with the higher symmetry space group, if they were separated from each other by $\Delta z = 1/2$. This is clearly not the case, since they form pairs with short and long Re–Re distances (225.7 and 348.6 pm) alternating along the *z* direction. One might speculate whether the space group *P*4/*ncc* with equal Re–Re distances might be adopted by these compounds at higher temperatures. In this case the high-temperature form could be a one-dimensional metallic conductor with delocalized metal–metal bonding. This high-temperature modification could then transform to the low-temperature form by a displacive phase transition, which in this case might be called a Peierls distortion, since delocalized transforms to localized Re–Re bonding. However, since the Re–Re bonding in Eu_2ReO_5 appears to be quite strong, it seems possible that rhenium pairs or clusters are already present in the liquid state and consequently the compound may crystallize directly in the lower symmetry form.

It is interesting that the compound Bi_2AuO_5, recently reported by Geb and Jansen (30), has exactly the higher symmetry structure just proposed for the potential high-temperature form of Eu_2ReO_5. These authors have discussed the structural relationships among Bi_2AuO_5, Bi_2CuO_4 (31), Bi_2PdO_4 (32), $La_4Au_2O_9$ (33), and $Bi_4Au_2O_9$ (30). The structure of the isotypic compounds Bi_2CuO_4 and Bi_2PdO_4 has the same space group (*P*4/*ncc*) as Bi_2AuO_5 with the same atomic positions, except that the oxygen atoms surrounded solely by bismuth atoms (corresponding to the O3 and O4 atoms of Eu_2ReO_5) are missing in

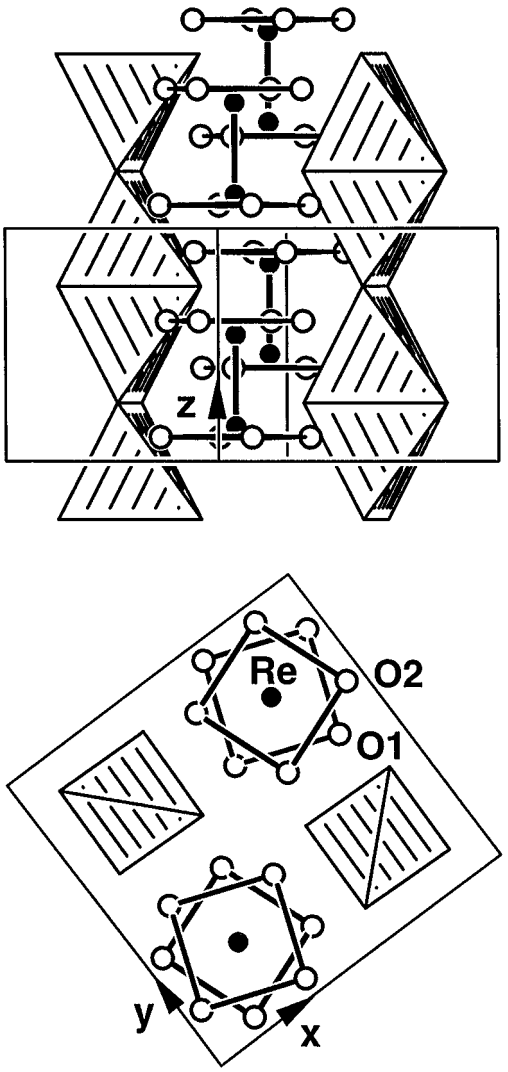

FIG. 4. The crystal structure of Eu_2ReO_5 emphasizing the chains of edge-sharing Eu_4O tetrahedra. The O3 and O4 atoms inside the tetrahedra are not shown. They alternate along the *z* axis.

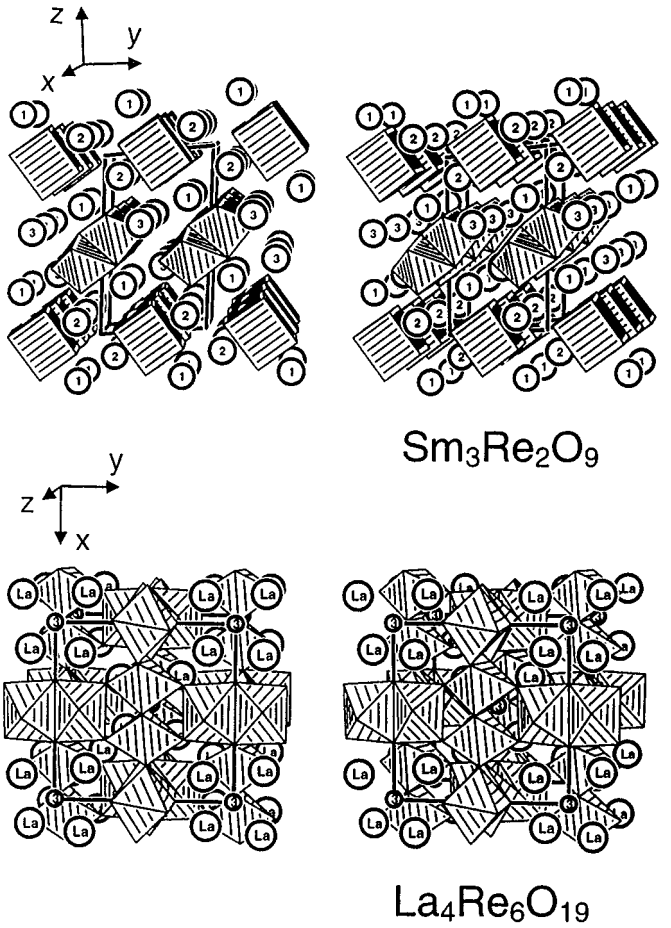

FIG. 5. Stereoplots of the structures of $Sm_3Re_2O_9$ and $La_4Re_6O_{19}$. The rare-earth atoms are shown as large spheres. The rhenium atoms (not shown) are situated within their oxygen polyhedra. In the structure of $La_4Re_6O_{19}$, the O3 atoms inside the tetrahedra formed by lanthanum atoms are emphasized.

Bi_2CuO_4 and Bi_2PdO_4. In $La_4Au_2O_9$ only every other oxygen atom is missing in each chain, whereas in $Bi_4Au_2O_9$ one-half of the chains of edge-sharing Bi_4 tetrahedra contains oxygen atoms and in the other chains the Bi_4 tetrahedra remain empty. The main difference between the structure of the rhenates Ln_2ReO_5 and the structures of the compounds just discussed can be seen in the pairing of the rhenium atoms, while the copper, palladium, and gold atoms have two equal or nearly equal distances to each other in their linear arrays.

The compounds Ln_2ReO_5 (Ln = Sm, Eu, Gd) have the same stoichiometry as La_2ReO_5 (17); however, the structure of La_2ReO_5 is different. It may be derived from the fluorite (CaF_2) structure. The oxygen environment of the Re_2 pairs in La_2ReO_5 consists of tetragonal prisms, whereas in Eu_2ReO_5 the Re_2 pairs are coordinated by tetragonal antiprisms of oxygen atoms. The rare-earth atoms have eight oxygen neighbors in both structures. In La_2ReO_5 the lanthanum atoms are situated in distorted cubes of oxygen atoms with La–O distances covering the range from 240.6(1) to 260.0(3) pm and with an average La–O distance of 252.9 pm. The europium atoms in Eu_2ReO_5 have a less regular oxygen environment (Fig. 3), with Eu–O distances varying between 228.4(4) and 264.0(6) pm and an average distance of 244.9 pm.

The other two structures of the rhenates reported here have already been discussed for $La_3Re_2O_9$ (18) and $La_4Re_6O_{19}$ (14, 15). Stereoplots of these structure types are shown in Fig. 5. Although the structure of $Sm_3Re_2O_9$ reported here is formally isotypic with that of $La_3Re_2O_9$, there are some remarkable differences in the coordination polyhedra of the three different rare earth sites of these two structures. To facilitate comparsions we have standardized

the structure of $La_3Re_2O_9$ using the program STRUCTURE TIDY (27). With this transformation the labels La1, La2, and La3 of Fig. 6 correspond to the atom designations La2, La3, and La1, respectively, of the previous investigation (18). In both compounds the coordination polyhedra of the *Ln*1 and *Ln*2 atoms are similar, with eight oxygen neighbors forming distorted cubes and *Ln*–O distances (with the average distances in parentheses) covering the ranges 242 to 272 pm (252.7 pm) for La1 (formerly La2), 242 to 268 pm (255.3 pm) for La2, 234 to 264 pm (245.3 pm) for Sm1, and 231 to 271 pm (247.5 pm) for Sm2. However, a ninth oxygen neighbor may be counted as belonging to the coordination of each lanthanum atom with La–O distances of 296 and 328 pm for the La1 and La2 atoms, respectively (Fig. 6), which are not that much greater than the other La–O distances, while the distances of the Sm1 and Sm2 atoms to the ninth oxygen atoms are even longer (302 and 335 pm) than the corresponding La–O distances. Therefore these ninth oxygen atoms can only marginally be counted as neighbors of the samarium atoms. The greatest difference between the structures of $La_3Re_2O_9$ and $Sm_3Re_2O_9$ occurs for the coordination polyhedra of the La3 and Sm3 atoms. The La3 atom has nine oxygen neighbors with La3–O distances between 240 and 282 pm (average 258.6 pm) and two additional oxygen atoms at 318 and 325 pm. In contrast, the Sm3 atom clearly has only eight close oxygen neighbors with Sm3–O distances between 232 and 268 pm (average 245.6 pm), whereas the three other corresponding oxygen atoms counted as belonging to the coordination of the La3 atoms are much farther away from the Sm3 atoms, with Sm3–O distances of 318, 319, and 333 pm. Obviously, the tendency for the larger coordination numbers of the lanthanum atoms is a consequence of their larger atomic size.

In the cubic structure of $La_4Re_6O_{19}$ (14, 15) adopted by the compounds $Ln_4Re_6O_{19}$ (Ln = La–Nd), the lanthanum atoms are situated on a threefold axis with 10 (3 + 3 + 3 + 1) oxygen neighbors at distances between 250.1 and 288.2 pm, and with an average distance of 265.0 pm. This distance compares well with the average La–O distance of 270.0 pm for the 11 oxygen neighbors of the La3 atom in $La_3Re_2O_9$ (18), considering the higher coordination number of the La3 atom in the 3:2:9 compound.

The most interesting structural aspects of the reduced oxorhenates concerns the rhenium–rhenium bonding. In all compounds of the present investigation the rhenium atoms form Re_2 pairs. In Table 9 we have summarized the oxidation state (formal charge) of the rhenium atoms, the Re–Re distances, and the coordination of the Re_2 pairs in the reduced rhenates of the rare-earth elements of the present investigation, together with data from the literature. It can be seen that the Re–Re distances correlate with the oxidation states and the resulting bond orders of the rhenium atoms within the Re_2 pairs. This indicates that the valence

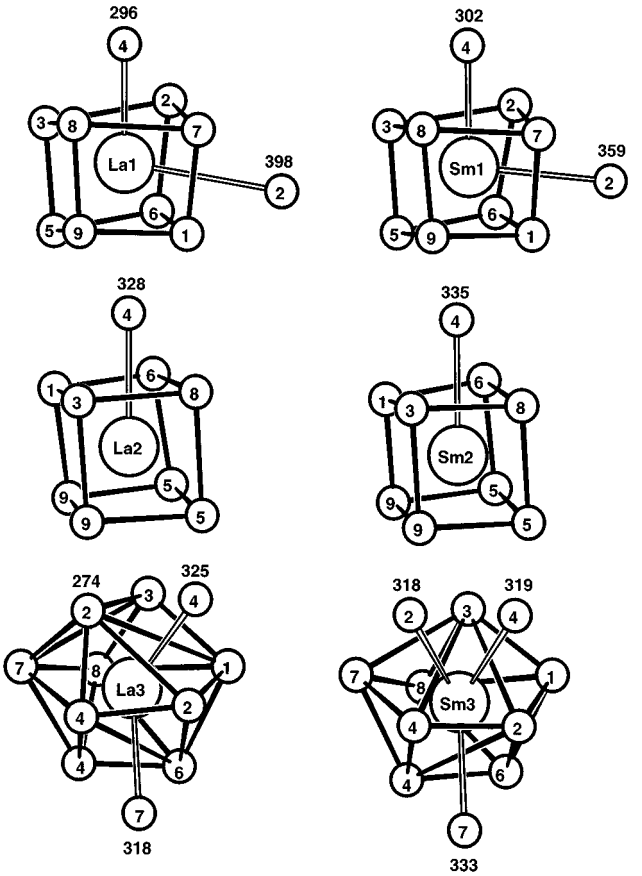

FIG. 6. Coordination of the rare earth atoms in $La_3Re_2O_9$ and $Sm_3Re_2O_9$. It can be seen, that some La–O distances (pm) are shorter than the corresponding Sm–O distances, although the two compounds may be considered to be isotypic. All near neighbors listed in Table 8 are shown. Both structures have been standardized by the program STRUCTURE TIDY (27). The atom labels La1, La2, and La3 used here, correspond to the atom designations La2, La3, and La1, respectively, of the original structure determination (18).

electrons of the rhenium atoms not needed for rhenium–oxygen bonding use their bonding potential to form Re–Re bonds.

The correlation between the formal bond orders and the bond lengths of the Re–Re distances is not linear, because the environments of the Re_2 pairs are also important. For small bond orders (1.5 to 2.67) and relatively high oxidation states (between +5.5 and +4.33) the rhenium atoms are situated in two edge-sharing oxygen octahedra. The bonding character of the Re–Re interactions is clearly indicated by the location of the rhenium atoms within their respective oxygen octahedra: the rhenium atoms are moved off the centers of their oxygen octahedra, thus approaching each other (Fig. 7). However, the Re–Re distances vary only between 248 pm for a bond order of 1.5 and 241 pm for a bond order of 2.67. The Re_2 pairs with higher bond orders have lower coordination numbers. They are situated in

TABLE 9
Rhenium–Rhenium Bond Lengths in Rare-Earth Rhenates[a]

Compound	Re oxidation state	Re–Re bond order	Re–Re distance (pm)	Re_2 pair coordination	Reference
$La_3Re_2O_{10}$	+5.5	1.5	248.4(1)	Edge-sharing octahedra	9
$La_3Re_2O_9$	+5	2	245.6(5)	Edge-sharing octahedra	18
$Dy_5Re_2O_{12}$	+4.5	2.5	244	Edge-sharing octahedra	11, 12
$Ho_5Re_2O_{12}$	+4.5	2.5	243.7(2)	Edge-sharing octahedra	13
$Sm_3Re_2O_9$	+5	2	242.3(1)	Edge-sharing octahedra	This work
$Nd_4Re_2O_{11}$	+5	2	242.1(1)	Edge-sharing octahedra	10
$La_4Re_6O_{19}$	+4.33	2.67	241.5(1)	Edge-sharing octahedra	14, 15
La_2ReO_5	+4	3	226.2	Tetragonal prism	17
$Sm_3Re_2O_9$	+4	3	225.1(1)	Tetragonal prism	This work
Eu_2ReO_5	+4	3	225.7(1)	Tetragonal antiprism	This work
Sm_2ReO_5	+4	3	225.1(1)	Tetragonal antiprism	20
Gd_2ReO_5	+4	3	224.5(1)	Tetragonal antiprism	This work
$La_3Re_2O_9$	+4	3	223.5(2)	Tetragonal prism	18

[a] The compounds are arranged with decreasing Re–Re distances. $La_3Re_2O_9$ and $Sm_3Re_2O_9$ are listed twice, because they contain two kinds of Re_2 pairs.

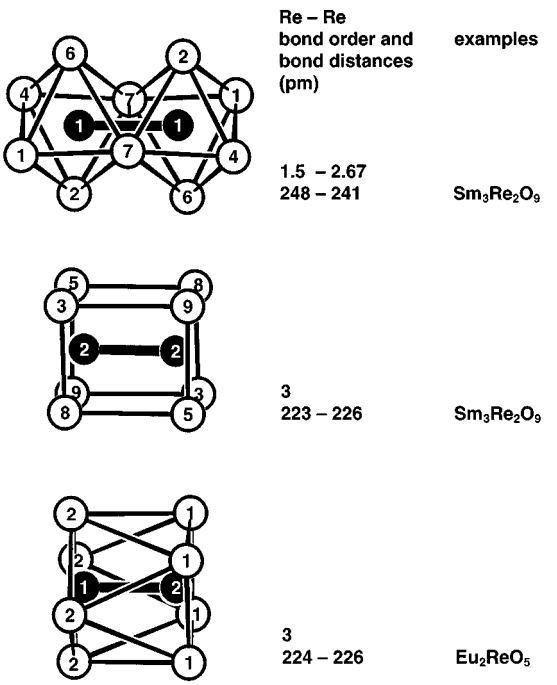

FIG. 7. Near-neighbor coordinations, bond order, and bond distances in rare-earth rhenium oxides with Re_2 pairs. The examples for the coordination polyhedra (with the atom designations represented by single-digit numbers) are taken from the presently reported structures of $Sm_3Re_2O_9$ and Eu_2ReO_5. At right, some data from Table 9 are summarized.

tetragonal prisms or antiprisms, and within these prisms each rhenium atom has only four close oxygen neighbors. These prisms allow considerable shorter Re–Re bonds. In all known examples, the rhenium atoms within the tetragonal prisms or antiprisms have the oxidation number +4, and consequently the bond order of the Re–Re bond is 3. The Re–Re distances of these Re_2 pairs vary between 223.5 and 226.2 pm (Table 9).

The magnetic properties of the compounds Eu_2ReO_5, Gd_2ReO_5, and $Ln_4Re_6O_{19}$ (Ln = La–Nd) reported here support this interpretation of the short Re–Re distances as beeing due to bonding Re–Re interactions. The experimentally determined effective moments μ_{exp} of the compounds with the magnetic lanthanoid atoms are all slightly smaller than the theoretical values μ_{eff}. Much higher experimental moments would be expected if the rhenium atoms were carrying localized magnetic moments.

In this context, the temperature-independent terms χ_0 resulting from our fits of the susceptibility data to the modified Curie–Weiss law are of interest. These values have large error limits for the three compounds $Ln_4Re_6O_{19}$ (Ln = Ce, Pr, Nd) because of the large moments of the rare-earth atoms and the limited temperature range of our Faraday balance. However, the SQUID data of Gd_2ReO_5 resulted in a value of $-170\ (\pm 90) \times 10^{-6}\,cm^3$/f.u. This value is comparible to the core diamagnetism of $-128 \times 10^{-6}\,cm^3$/f.u., calculated from the increments (Ln^{3+}: −20, Re^{4+}: −28, and O^{2-}: $-12 \times 10^{-6}\,cm^3$/atom) given by Klemm (34, 35). Thus, within the experimental error limits the rhenium atoms make no paramagnetic contributions to the susceptibility in Gd_2ReO_5.

The most reliable result for a χ_0 value was obtained for $La_4Re_6O_{19}$, because in this compound the La^{3+} ions do not carry magnetic moments. The magnetic susceptibility of this compound is practically zero within the relatively small error limits of $\pm 20 \times 10^{-6}\,cm^3$/f.u. Therefore, in $La_4Re_6O_{19}$ the rhenium atoms seem to have a small paramagnetic contribution to the susceptibility, which just compensates the core diamagnetism. The latter amounts to $476 \times 10^{-6}\,cm^3$/f.u., calculated from the increments given above (34, 35).

The compounds reported here are all black. We have not determined their electrical conductivities; however, we do not expect them to show metallic behavior, since we believe their valence electrons to be engaged in localized

rhenium–oxygen and rhenium–rhenium bonding. Thus, we assume these compounds to be semiconductors with relatively small band gaps to rationalize their black color.

A remarkable inconsistency with the structural systematics of the reduced rhenates of the rare-earth elements just discussed is the structure recently reported for Sm_3ReO_7 (36). In contrast to the other reduced rhenates, it does not contain any short Re–Re bonds, although the rhenium atoms have the oxidation number +5. This structure is also remarkable because the average Sm–O distance of one samarium atom with eightfold oxygen coordination is 253.3 pm, which is considerably greater than the average Sm–O distances of 245.3, 247.5, and 245.6 pm found in the present investigation for the eight short Sm–O distances of the Sm1, Sm2, and Sm3 atoms in $Sm_3Re_2O_9$. On the other hand, the average Re–O distance of 194.5 pm reported for the octahedrally coordinated rhenium(V) atom of Sm_3ReO_7 is considerably greater than the average Re(VII)–O distances of between 187.0 and 189.7 pm found for seven different $Re(VII)O_6$ octahedra in $Ca_5Re_2O_{12}$ (37), $Sr_5Re_2O_{12}$ (37), and $Ca_{11}Re_4O_{24}$ (38), thus reflecting the lower oxidation state of rhenium in Sm_3ReO_7.

An interesting difference can be observed by comparing the structural chemistry of the reduced rhenates with that of reduced molybdates. At least in general, the rhenium atoms in the reduced rhenates form pairs with short Re–Re bond distances, indicating multiple-bond character. In contrast, the molybdenum atoms in the reduced molybdates of the rare-earth elements form molybdenum clusters, where less than two valence electrons are to be counted for each Mo–Mo interaction. Examples are the chains of edge-sharing Mo_6 octahedra in $Ho_4Mo_4O_{11}$, where the molybdenum atoms have the average oxidation number +2.5 (39), the Mo_{10} clusters in $GdMo_5O_8$ with molybdenum in the average oxidation state +2.6 (40), the Mo_8 and Mo_{24} clusters in $La_5Mo_{32}O_{54}$ (average Mo: +2.906) (41), the Mo_{10} clusters in $Ce_{16}Mo_{21}O_{56}$ (42) and $Nd_{16}Mo_{21}O_{56}$ (43), where the average molybdenum atoms have a formal charge of +3.05, and the various Mo_8 clusters in the structures of the series RMo_8O_{14} (R = La–Nd, Sm) with the average oxidation number +3.125 for molybdenum (44–46). However, when the molybdenum atoms carry a higher formal charge, they also form Mo_2 pairs, as was found for the structures of $La_2Mo_2O_7$ (47), $La_5Mo_4O_{16}$ (48), $Y_5Mo_2O_{12}$ (49), and $La_4Mo_2O_{11}$ (50), where the average molybdenum atoms carry formal charges of +4, +4.25, +4.5, and +5, respectively. Apparently, this difference in the structural chemistry of the reduced molybdates and rhenates has to do with the fact that the molybdates are frequently obtained in a less reduced form. We wonder if less highly reduced rare earth rhenium oxides can be synthesized that will have clusters of rhenium atoms similar to the clusters in the molybdenum oxides with lower oxidation states.

ACKNOWLEDGMENTS

We thank Mrs. J. Nowitzki, Dr. M. Reehuis, Dr. Th. Vomhof, and Dipl.-Phys. M. Wolff for the magnetic susceptibility measurements with the Faraday balance and the SQUID magnetometer and for discussions of these data. We also acknowledge Mr. K. Wagner for the work with the scanning electron microscope. We are indebted to Dr. H. G. Nadler (H. C. Starck) and Dr. G. Höfer (Heraeus Quarzschmelze) for generous gifts of rhenium metal and silica tubes. This work was also supported by the Deutsche Forschungsgemeinschaft, the Fonds der Chemischen Industrie, and the International Centre for Diffraction Data.

REFERENCES

1. O. Muller and R. Roy, *Mater. Res. Bull.* **4,** 349 (1969).
2. G. Baud, J.-P. Besse, and R. Chevalier, *J. Solid State Chem.* **38,** 186 (1981).
3. G. Baud, J.-P. Besse, R. Chevalier, and M. Gasperin, *J. Solid State Chem.* **29,** 267 (1979).
4. A. R. Rae-Smith, A. K. Cheetham, and H. Fuess, *Z. Anorg. Allg. Chem.* **510,** 46 (1984).
5. J.-P. Besse, M. Bolte, G. Baud, and R. Chevalier, *Acta Crystallogr. B* **32,** 3045 (1976).
6. V. E. Plyushchev and M. B. Varfolomeev, *Russ. J. Inorg. Chem.* **10,** 564 (1966).
7. V. I. Ivanov, M. B. Varfolomeev, and V. E. Plyushchev, *Kristallografiya* **13,** 167 (1968).
8. V. N. Khrustalev, M. B. Varfolomeev, N. B. Shamrai, Yu. T. Struchkov, and A. P. Pisarevskii, *Koord. Khim* **19,** 871 (1993).
9. C. C. Torardi and A. W. Sleight, *J. Less-Common Met.* **116,** 293 (1986).
10. K.-A. Wilhelmi, E. Lagervall, and O. Muller, *Acta Chem. Scand.* **24,** 3406 (1970).
11. G. Baud, J.-P. Besse, M. Capestan, and R. Chevalier, *Ann. Chim. (Paris)* **7,** 615 (1982).
12. G. Baud, J.-P. Besse, R. Chevalier, and M. Gasperin, *Mater. Chem. Phys.* **8,** 93 (1983).
13. D. H. Heumannskämper and W. Jeitschko, *Z. Kristallogr.* **178,** 99 (1987).
14. N. L. Morrow and L. Katz, *Acta Crystallogr. B* **24,** 1466 (1968).
15. J. M. Longo and A. W. Sleight, *Inorg. Chem.* **7,** 108 (1968).
16. M. S. Schriewer, D. H. Heumannskämper, H. A. Mons, and W. Jeitschko, *Acta Crystallogr. A* **46,** Supplement, C-275 (1990).
17. K. Waltersson, *Acta Crystallogr. B* **32,** 1485 (1976).
18. J.-P. Besse, G. Baud, R. Chevalier, and M. Gasperin, *Acta Crystallogr. B* **34,** 3532 (1978).
19. D. H. Heumannskämper and W. Jeitschko, *Z. Kristallogr.* **182,** 132 (1988).
20. G. Wltschek, H. Paulus, H. Ehrenberg, and H. Fuess, *J. Solid State Chem.* **132,** 196 (1997).
21. K. Yvon, W. Jeitschko, and E. Parthé, *J. Appl. Crystallogr.* **10,** 73 (1977).
22. J. H. Van Vleck, "The Theory of Electric and Magnetic Susceptibilities." Oxford Univ. Press, Oxford, 1932.
23. W. Jeitschko and M. Reehuis, *J. Phys. Chem. Solids* **48,** 667 (1987).
24. B. A. Frenz and Associates Inc. and Enraf-Nonius, SDP (Structure Determination Package), Version 3, College Station (Texas) and Delft (Holland), 1985.
25. M. Eitel and H. Bärnighausen, "Kleinst-Quadrat-Programm zur Verfeinerung von Datensätzen verzwillingter oder verdrillingter Kristalle," Universität Karlsruhe, Germany, 1986.
26. G. M. Sheldrick, "SHELXL-92, A Program for Crystal Structure Refinement," Beta Version. Universität Göttingen, Germany, 1992.
27. L. M. Gelato and E. Parthé, *J. Appl. Crystallogr.* **20,** 139 (1987).

28. D. H. Heumannskämper, Doctoral Thesis, Universität Münster, Germany, 1989.
29. M. S. Schriewer, Doctoral Thesis, Universität Münster, Germany, 1992.
30. J. Geb and M. Jansen, *J. Solid State Chem.* **122,** 364 (1996).
31. J.-C. Boivin, J. Tréhoux, and D. Thomas, *Bull. Soc. Fr. Minéral. Cristallogr.* **99,** 193 (1976).
32. P. Conflant, J.-C. Boivin, and D. Thomas, *Rev. Chim. Minér.* **14,** 249 (1977).
33. M. Ralle and M. Jansen, *J. Alloys Compd.* **203,** 7 (1994).
34. W. Klemm, *Z. Anorg. Allg. Chem.* **246,** 347 (1941).
35. A. Weiss and H. Witte, "Magnetochemie." Verlag Chemie, Weinheim, 1973.
36. G. Wltschek, H. Paulus, I. Svoboda, H. Ehrenberg, and H. Fuess, *J. Solid State Chem.* **125,** 1 (1996).
37. H. A. Mons, M. S. Schriewer, and W. Jeitschko, *J. Solid State Chem.* **99,** 149 (1992).
38. W. Jeitschko, H. A. Mons, U. Ch. Rodewald, and M. H. Möller, *Z. Naturforsch.* **53b,** 31 (1998).
39. P. Gougeon, P. Gall, and R. E. McCarley, *Acta Crystallogr. C* **47,** 1585 (1991).
40. P. Gougeon, P. Gall, and M. Sergent, *Acta Crystallogr. C* **47,** 421 (1991).
41. P. Gall, L. Toupet, and P. Gougeon, *Acta Crystallogr. C* **49,** 1580 (1993).
42. P. Gall and P. Gougeon, *Acta Crystallogr. C* **49,** 659 (1993).
43. P. Gall and P. Gougeon, *Z. Kristallogr.* **213,** 1 (1998).
44. H. Leligny, M. Ledesert, Ph. Labbé, B. Raveau, and W. H. Carroll, *J. Solid State Chem.* **87,** 35 (1990).
45. P. Gougeon and R. E. McCarley, *Acta Crystallogr. C* **47,** 241 (1991).
46. G. Kerihuel and P. Gougeon, *Acta Crystallogr. C* **51,** 787 (1995).
47. A. Moini, M. A. Subramanian, A. Clearfield, F. J. DiSalvo, and W. H. McCarroll, *J. Solid State Chem.* **66,** 136 (1987).
48. M. Ledesert, Ph. Labbé, W. H. Carroll, H. Leligny, and B. Raveau, *J. Solid State Chem.* **105,** 143 (1993).
49. C. C. Torardi, C. Fecketter, W. H. McCarroll, and F. J. DiSalvo, *J. Solid State Chem.* **60,** 332, (1985).
50. P. Gall and P. Gougeon, *Acta Crystallogr. C* **48,** 1915 (1992).